Data-driven Estimation of Probabilistic Constraints for Network-safe Distributed Energy Resource Control

Sunho Jang, Necmiye Ozay, Johanna L. Mathieu

Abstract— Distribution network safety should not be compromised when distributed energy resources (DERs) provide balancing services to the grid. Often DER coordination is achieved through an aggregator. Thus, it is necessary to develop network-safe coordination schemes between the distribution network operator (i.e., the utility) and the aggregator. In this work, we introduce a framework in which the utility computes and sends a constraint set on the aggregators' control commands to the DERs. We propose a policy to adjust the charging/discharging power of distributed batteries, which allows them to be incorporated into the framework. Also, we propose a data-driven approach for the utility to construct a constraint set with probabilistic guarantees on network safety. The proposed approach allows the DERs to provide network-safe services without heavy communication requirements or invasion of privacy. Numerical simulations with distributed batteries and thermostatically controlled loads show that the proposed approach achieves the desired level of network safety and outperforms two benchmark algorithms.

I. INTRODUCTION

As penetrations of variable and uncertain renewable energy sources increase, the grid needs more resources that can help balance supply and demand. Distributed Energy Resources (DERs) connected to the distribution system, such as batteries, flexible electric loads, and curtailable renewable resources, can provide grid balancing services, which in turn can improve the reliability, reduce the operating cost, and reduce the environmental impact of the electric power system.

Strategies to coordinate DERs must not only provide effective balancing services, but should also consider distribution network safety. Indiscriminate operation of DERs might threaten the safety of the distribution network by, for example, inducing voltage or current constraint violations [1]; this problem usually occurs when the power consumption/production of a portion of the network is excessively high or low. Thus, DERs should be controlled in such a way that network safety is guaranteed. Some work, e.g., [2]–[4], has proposed centralized network-safe control algorithms for DERs. These approaches assume that the distribution network operator (i.e., the utility), which has access to detailed information about the distribution network (e.g., its topology and line parameters), can directly control the DERs. However, in U.S. competitive electricity markets, it is becoming more common for a third-party (i.e., non-utility) DER aggregator to coordinate DERs to

provide balancing services. Aggregators may have limited or no direct information about the distribution network. This means that the aggregator alone cannot coordinate DERs while ensuring network safety.

The US Federal Energy Regulatory Commission (FERC) has recognized the potential network safety challenges associated with third-party aggregators coordinating DERs connected to utility-operated networks [1] and has begun to provide some guidance on operational coordination between DER aggregators, utilities, and market coordinators via FERC Order No. 2222 [5]. However, FERC has left the detailed development of coordination architectures to the independent systems operators (ISOs), which are still in the process of responding to FERC Order No. 2222, and so currently the best architectures for aggregator-utility coordination are unclear. In addition to enabling adequate balancing services and network safety, the architectures should ensure private information stays private (e.g., network information maintained by the utility, proprietary DER coordination strategies developed by the aggregator, and some real-time DER state information such as home indoor temperatures) and, ideally, require only minimal communication between the entities.

Motivated by the above issues, in our recent work [6], we introduced a coordination strategy to provide network-safe balancing services with thermostatically controlled loads (TCLs). In particular, this approach guarantees that the probability of network safety at each time step is above a desired value with a desired confidence level. We assume both the uncontrollable load in the network and the TCL response to the control command are uncertain. In our framework, the utility does not provide private network information to the aggregator, and the communication requirements between the entities (aggregator, utility, and the DERs) are light. Instead, we assume that the utility computes a constraint set on the aggregator's control commands and sends it to the aggregator so that, as long as the aggregator chooses its command from the set, safety is guaranteed with high probability. However, this earlier work only considers TCLs and so it cannot utilize the potential flexibility that can be provided by other types of DERs.

In this paper, we extend the framework in [6] by considering batteries as an additional type of DER. In particular, the main contribution of this paper is to provide a control policy to adjust the charging/discharging power of batteries under the same type of control command as that proposed in [6]. We also extend the constraint construction algorithm in [6] to be more general.

Some previous work has considered similar frameworks as ours, in which a utility and an aggregator coordinate to enable network-safe grid balancing services from DERs. Ref. [7] proposes two coordination approaches between the utility and the aggregator – an *aggregator-centric framework*, in which the aggregator receives constraints from the utility and then directly controls DERs, and a *utility-centric framework*, in which the aggregator control commands are intercepted and blocked/modified by the utility if they could lead to network safety violations. However, it does not propose a network-safe controller for the aggregator-centric case, which is the case we consider in this paper. Also, two different strategies for network-safe TCLs coordination are proposed in [8]; however, these approaches require more degrees of freedom in control (i.e., higher dimensional command) than ours and assume deterministic uncontrollable loads. Ref. [9] also proposed a safety-guaranteed and non-disruptive TCL coordination algorithm under an aggregator-centric framework; however, the approach assumes that the aggregator has access to TCL state information (e.g., for an air conditioner this would corresponding to real-time indoor temperatures and compressor on/off states), which participants may not wish to share. Also the paper assumes network-safe aggregate power bounds are available from the utility, but does not explore how to derive them.

Many papers have proposed methods to construct *safe operating regions* where, as long as the DERs are operated within it, the safety of the network is guaranteed. Some work from Australia proposes coordination schemes in which the utility constructs *operating envelopes* [10]–[12] and sends them to prosumers or aggregators; however, the constructed operating envelopes are node-specific and are useful only when the aggregator's control actions are also node-specific, again requiring additional communication beyond what is required in our approach. Ref. [13]–[15] construct convex inner approximations of safe operating regions, which enables the incorporation of safe operating regions into convex optimal power flow (OPF) problems. However, the size of the inner approximation can be small, especially for networks with a large number of nodes, resulting in excessively conservative operation of DERs.

The organization of the paper is as follows. Section II introduces the coordination framework and Section III develops the battery control strategy. Section IV extends the constraint set construction algorithm for satisfying a chance constraint on network safety. Section V illustrates the result of a case study.

Notation: We denote by $\mathbb{N}$, $[N]$, $[N]_0$ the set of natural numbers, $\{1, \ldots, N\}$, and $\{0, 1, \ldots, N\}$, respectively. We write the n-dimensional Euclidean space as $\mathbb{R}^n$. The jth element of the vector $\boldsymbol{y}$ is denoted by y_j. $\mathcal{N}(\mu, \sigma^2)$ refers to the normal distribution with mean μ and variance σ^2. We denote random variables with capital letters, and their realizations with tilde on top of the corresponding lowercase letter. All variables other than random variables (except matrices) are denoted by lowercase letters.
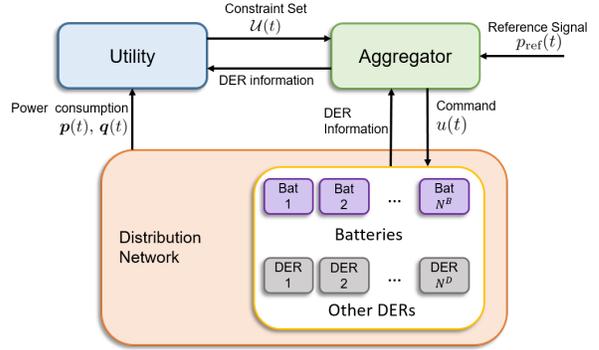

Fig. 1: Coordination between the utility and the aggregator in our framework.

II. UTILITY-AGGREGATOR COORDINATION FRAMEWORK

We consider a problem of controlling a collection of DERs to provide balancing service to the grid while ensuring distribution network safety. Similar to [6], a discrete-time coordination scheme between the utility and the aggregator is considered, where the length of each time step is denoted by Δt. The coordination scheme is as follows.

1) The aggregator receives constraint set $\mathcal{U}(t)$ from the utility corresponding to its DER control command $u(t)$. It also receives a reference signal $p_{\text{ref}}(t)$ from the ISO, for example, a (scaled and biased) frequency regulation signal.
2) The aggregator broadcasts $u(t)$ to all participating DERs in the network.
3) Based on the received $u(t)$, the DERs may adjust their power consumption/production.
4) The utility observes the real and reactive power consumption $\boldsymbol{p}(t)$, $\boldsymbol{q}(t)$ at each network node and computes the one-step ahead constraint set $\mathcal{U}(t+1)$ on the one-step ahead input $u(t+1)$.

Fig. 1 illustrates this scheme.

To achieve light communication requirements, we assume that $u(t)$ is one-dimensional, i.e., $u(t) \in \mathbb{R}$, and so the same value can be broadcast to all DERs. However, DERs may respond to $u(t)$ differently, and the way in which each DER acts on $u(t)$ depends on its type. For example, in [6] the command $u(t)$ is the desired probability of a TCL (which cycles on/off to maintain temperature within a dead-band) to switch its mode. Each TCL draws a random number to determine whether or not it should switch. In this paper, in Section III-B, we show how the same input $u(t)$ can be interpreted by batteries to adjust their power consumption/production. Note that, within this scheme, the power consumption/production of each DER cannot be individually adjusted by the aggregator, which means the aggregator has a low degree of freedom in control.

The responsibility of the aggregator is to maximize the quality of the balancing service by broadcasting an appropriate control command $u(t)$ to all participating DERs. Hence, $u(t)$ should be chosen in such a way that the aggregate power consumption/production of the participating DERs is as close to the reference signal $p_{\text{ref}}(t)$ as possible. However, the

aggregator's choice of $u(t)$ might risk network safety and so it must coordinate with the utility. To keep the network safe, the utility sends the aggregator a one-step ahead constraint set $\mathcal{U}(t+1)$ on the command $u(t+1)$. Then, the aggregator must choose $u(t+1)$ from the constraint set $\mathcal{U}(t+1)$; the optimal control command is the element of $\mathcal{U}(t+1)$ that achieves the aggregate power consumption/production of the participating DERs closest to the reference signal $p_{\text{ref}}(t+1)$.[1]

To make this procedure possible, the utility should be able to predict the effect of a one-step ahead input $u(t+1)$ on network safety and be able to compute the one-step ahead constraint set $\mathcal{U}(t+1)$. We introduce a method for the utility to compute the one-step ahead constraint set $\mathcal{U}(t+1)$ in Section IV. We assume that the utility uses the following information.

1) Real-time real and reactive power consumption $p(t)$, $q(t) \in \mathbb{R}^n$ at every network node, obtainable from smart meter measurements configured to transmit their measurements in real-time.[2]
2) Joint probability distribution $f^t_{P^L, Q^L}$ of real and reactive power consumption P^L, Q^L of the non-participating DERs and loads. We assume this can be obtained by leveraging an energy disaggregation technique to separate historical power consumption data into the power consumption from i) participating DERs and ii) non-participating DERs and loads.

While ensuring network safety requires constraints on nodal voltages, line currents, transformer temperatures, voltage unbalance, and so on, in this paper, we consider only under-voltage violations for simplicity, though our approach can be extended to handle other constraints. Specifically, we wish to keep the probability of network safety (i.e., no under-voltage violations) over a desired probability $1 - \epsilon$. Let n be the number of the nodes in the distribution network other than the substation, and $V_j(t+1)$ be the anticipated one-step ahead voltage at node j under the one-step ahead input $u(t+1)$. Then, the formal problem statement is as follows.

Problem 1. *Given the desired safety probability $1 - \epsilon$, the observed $p(t)$, $q(t)$ at each node, and the joint pdf $f^t_{P^L, Q^L}$, $f^{t+1}_{P^L, Q^L}$, compute a one-step ahead constraint set $\mathcal{U}(t+1)$ on the one-step ahead command $u(t+1)$ such that the following chance constraint holds if $u(t+1) \in \mathcal{U}(t+1)$*

$$Pr\left(\min_{j \in [n]} V_j(t+1) \geq \underline{v}\right) \geq 1 - \epsilon. \qquad (1)$$

[1]While ideally the aggregator should not offer more balancing services than the distribution network can support, it is difficult for the aggregator to determine a feasible market offer in advance because the maximum feasible quantity of balancing services is a function of the actions of other resources (loads and renewables) on the network. Therefore the aggregator (and/or utility) must forecast these things to enable the aggregator to develop their market offer. In this paper, we consider the case in which the quantity of balancing services provided by the aggregator (i.e., the kW range of the real-time reference signal $p_{\text{ref}}(t)$) has already been set in the market but deviations from forecasts have lead to the need to further constrain balancing service delivery to ensure network safety.

[2]Most smart meters in the US can capture real-time measurements but only transmit data back to the utility once/day.

III. INCORPORATING BATTERIES INTO THE FRAMEWORK

In this section, we introduce the battery model and propose a policy for the battery to adjust its charging/discharging power given the aggregator's command $u(t)$. This policy allows us to incorporate batteries into our utility-aggregator coordination framework. For simplicity, we assume that the battery is operated at unity power factor, i.e., it does not consume reactive power.

A. Battery dynamics and constraints

We first introduce the dynamics of a battery's state of charge (SoC) and the constraints on a battery's SoC and charging/discharging power. We let n^{B} be the number of the participating batteries in the network. For each $i \in [n^{\text{B}}]$, the SoC dynamics of the ith battery are

$$e^i(t+1) = e^i(t) + \eta^i_{\text{c}} p^i_{\text{c}}(t)\Delta t + \frac{p^i_{\text{d}}(t)}{\eta^i_{\text{d}}}\Delta t, \qquad (2)$$

where $e^i(t)$ is the energy state (i.e., the SoC times the energy capacity $\overline{e}^i$ of the battery), $p^i_{\text{c}}(t)$ and $p^i_{\text{d}}(t)$ are the charging and discharging power, and η^i_{c} and η^i_{d} are the charging and discharging efficiency of the ith battery, respectively. Then, we define the net power consumption of the battery as

$$p^i(t) = p^i_{\text{c}}(t) + p^i_{\text{d}}(t).$$

We assume a battery is unable to charge and discharge simultaneously, and so $p^i_{\text{c}}(t) \cdot p^i_{\text{d}}(t) = 0$.

The bounds on the energy state and the charging/discharging power are

$$0 \leq e^i(t) \leq \overline{e}^i, \quad 0 \leq p^i_{\text{c}}(t) \leq \overline{p}^i, \quad \underline{p}^i \leq p^i_{\text{d}}(t) \leq 0, \quad (3)$$

where $\overline{p}^i > 0$ and $\underline{p}^i < 0$ are the maximum charging and discharging power of the ith battery. Note that usually $\underline{p}^i = -\overline{p}^i$.

B. Battery power adjustments

In this section, we propose a policy for the batteries to adjust their net power consumption $p^i(t)$ according to the aggregator's control command $u(t)$. We let $u(t)$ take values in the range $[-1, 1]$. In [6], this command is interpreted by TCLs as the probability to switch modes. That is, if $u(t)$ is positive (negative, respectively), each TCL that is currently OFF (ON) switches ON (OFF) with probability $u(t)$ ($|u(t)|$) by drawing a random number and comparing it to the $u(t)$. As a result, the anticipated increase/decrease in the aggregate power consumption of the TCLs is $|u(t)|$ times the maximum increase/decrease that is possible. The policy we propose for batteries makes the aggregate power consumption/production of batteries behave similarly under the same command $u(t)$. Thus, if the batteries follow the proposed policy, the probability of network safety is guaranteed when both batteries and TCLs are incorporated into our framework.

Specifically, we assume the batteries react to the aggregator's command $u(t)$ using the following policy.
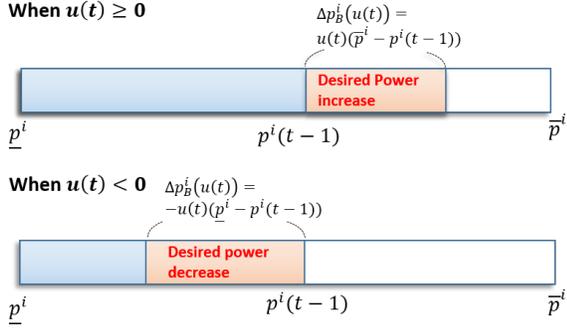
Fig. 2: The desired power variation Δp_B^i under the command $u(t)$. The blue area on the top band shows the net power consumption of the batteries in the last time step. The orange areas shows the power increase (top band) or decrease (bottom band).

1) The absolute value of the command $u(t)$ represents the desired *ratio* of net power consumption increase/decrease a battery should implement compared to what it can maximally achieve.
2) The sign of the command $u(t)$ indicates the direction of the change in net power consumption; we want the net power consumption of the battery to increase when $u(t)$ is positive, and to decrease when it is negative.

Mathematically, the maximum and minimum possible net power consumption adjustments of the ith battery are $\Delta p_{\max}^i = \overline{p}^i - p^i(t)$, $\Delta p_{\min}^i = \underline{p}^i - p^i(t)$, respectively. Therefore, according to the proposed battery control policy, the desired power variation Δp_B^i under input $u(t)$ is

$$\Delta p_B^i(u(t)) = \begin{cases} u(t)\Delta p_{\max}^i, & \text{if } u(t) \geq 0, \\ -u(t)\Delta p_{\min}^i, & \text{if } u(t) < 0. \end{cases}$$

Note that, since $\Delta p_{\max}^i \geq 0$, $\Delta p_{\min}^i \leq 0$, the value of $\Delta p_B^i(u(t))$ is positive when $u(t)$ is non-negative and negative when $u(t)$ is negative. Fig. 2 shows how $\Delta p_B^i(t)$ is computed.

However, the desired net power consumption $p_{\text{des}}^i(t) = p^i(t-1) + \Delta p_B^i(u(t))$ might not be achievable if a battery is nearly fully charged or nearly empty. If $p^i(t)$ is larger than $\frac{\overline{e}^i - e^i(t)}{\eta_c^i \Delta t}$, then $e^i(t+1)$ becomes larger than $\overline{e}^i$. Similarly, $e^i(t+1)$ becomes smaller than 0 if $p^i(t)$ is smaller than $-\frac{\eta_d^i e^i(t)}{\Delta t}$. Thus, $p^i(t)$ should be between $-\frac{\eta_d^i e^i(t)}{\Delta t}$ and $\frac{\overline{e}^i - e^i(t)}{\eta_c^i \Delta t}$ to satisfy the energy state constraint in (3). Considering this, we adjust $p^i(t)$ using

$$p^i(t) = \begin{cases} \min\left\{p_{\text{des}}^i(t), \frac{\overline{e}^i - e^i(t)}{\eta_c^i \Delta t}\right\}, & \text{if } u(t) \geq 0, \\ \max\left\{p_{\text{des}}^i(t), -\frac{\eta_d^i e^i(t)}{\Delta t}\right\}, & \text{if } u(t) < 0. \end{cases} \quad (4)$$

If all of the participating batteries adjust their charging/discharging power using the proposed policy, then the increase/decrease in the batteries' aggregate net power consumption behaves similarly to the increase/decrease in the TCLs' aggregate power consumption, as described in [6], under the same control command $u(t)$. Hence, the aggregator can simultaneously control batteries and TCLs by broadcasting the same command $u(t)$ to all participating DERs. One small difference in the implementation of the control policies

is that the TCLs switch probabilistically and so their response is uncertain (where the amount of uncertainty decreases with the size of the TCL population). In contrast, the batteries change their net power consumption deterministically.

Note that we can design control policies for other types of DERs in similar ways so that the increase/decrease of their aggregate net power consumption is the portion $|u(t)|$ of their maximum possible increase or decrease. This would allow the aggregator to control a heterogeneous aggregation of DERs with a simple low-degree-of-freedom controller to provide balancing services and achieve network safety with probabilistic guarantees.

IV. CONSTRUCTING PROBABILISTICALLY-SAFE INPUT CONSTRAINTS

In this section, we introduce an approach for the utility to construct a one-step ahead constraint set $\mathcal{U}(t+1)$ on the aggregator's control command $u(t+1)$ for the satisfaction of the chance-constraint (1). The construction process follows our recent work [6] but here we incorporate batteries as controllable DERs in addition to TCLs. We first describe how the probability of network safety is computed under a given one-step ahead control command $u(t+1)$. Then, we state a theorem on the confidence interval for the success probability of a Bernoulli random variable, which we will use for constraint construction. Finally, we explain how we can construct the one-step ahead constraint set $\mathcal{U}(t+1)$.

A. One-step ahead probability of network safety

In this section, we explain how to model the probability of network safety in the next time step given a one-step ahead aggregator control command $u(t+1) = u$. We first model the anticipated one-step ahead power consumption and voltage at each node as random variables whose probability distributions are dependent on u. Then, we show that the anticipated one-step ahead probability of network safety can be modeled as the success probability of a Bernoulli random variable.

We first denote by $\boldsymbol{p}^{B+}(u) \in \mathbb{R}^n$ the anticipated one-step ahead net power consumption of the batteries connected to each node under input $u(t+1) = u$. Then, each element of $\boldsymbol{p}^{B+}(u)$ is

$$p_j^{B+}(u) = \begin{cases} \sum_{i \in \mathcal{I}_j^B} \min\left\{p_{\text{des}}^{i+}, \frac{\overline{e}^i - e^{i+}}{\eta_c^i \Delta t}\right\}, & \text{if } u \geq 0, \\ \sum_{i \in \mathcal{I}_j^B} \max\left\{p_{\text{des}}^{i+}, -\frac{\eta_d^i e^{i+}}{\Delta t}\right\}, & \text{if } u < 0, \end{cases} \quad (5)$$

where $\mathcal{I}_j^B$ is the set of indices of the batteries connected to node j, $p_{\text{des}}^{i+} = p^i(t) + \Delta p_B^i(u(t+1))$ is the anticipated one-step ahead desired net power consumption, and e^{i+} is the anticipated one-step ahead energy state obtained from (2) under input $u(t+1) = u$.

Let $\boldsymbol{P}^+(u)$ and $\boldsymbol{Q}^+(u) \in \mathbb{R}^n$ be the anticipated total real and reactive power consumption at each node at the next time step under the input u, i.e.,

$$\begin{aligned} \boldsymbol{P}^+(u) &= \boldsymbol{p}^{B+}(u) + \boldsymbol{p}^{D+}(u) + \boldsymbol{P}^{L+} \\ \boldsymbol{Q}^+(u) &= \boldsymbol{q}^{D+}(u) + \boldsymbol{Q}^{L+}, \end{aligned} \quad (6)$$

where $\boldsymbol{p}^{\mathrm{D}+}(u)$ and $\boldsymbol{q}^{\mathrm{D}+}(u)$ are the anticipated one-step ahead real and reactive power consumption of the participating DERs other than the batteries under the input u, and $\boldsymbol{P}^{\mathrm{L}+}$ and $\boldsymbol{Q}^{\mathrm{L}+}$ are the anticipated one-step ahead real and reactive power consumption of the non-participating DERs and loads, where $\boldsymbol{P}^{\mathrm{L}+}$ and $\boldsymbol{Q}^{\mathrm{L}+}$ are random variables whose joint distribution is $f_{\boldsymbol{P}^{\mathrm{L}},\boldsymbol{Q}^{\mathrm{L}}}^{t+1}$.

In this work, we assume that the utility can compute the anticipated one-step ahead power consumption $\boldsymbol{p}^{\mathrm{D}+}(u)$. In particular, for the case study in Section V, we assume that all the participating DERs other than the batteries are TCLs so that $\boldsymbol{p}^{\mathrm{D}+}(u)$ can be obtained using the results in [6]. Assuming that the average power consumption of the participating DERs at each node increases with u, $\boldsymbol{p}^{\mathrm{D}+}(u)$, $\boldsymbol{q}^{\mathrm{D}+}(u)$, and $\boldsymbol{p}^{\mathrm{B}+}(u)$ are increasing functions with respect to u.

Now, we show how to model the anticipated one-step ahead voltage $\boldsymbol{V}^{+}(u) \in \mathbb{R}^n$ under input $u(t+1) = u$ as a random variable. Let r_j and x_j denote the resistance and reactance of the branch ending at node j, and let $e(j)$ denote the parent node and $c(j)$ the set of child nodes of node j. Then, assuming the distribution network is radial, the following *DistFlow equations* [16] hold

$$
\begin{aligned}
p_j^{\mathrm{b}} &= \sum_{k \in c(j)} p_k^{\mathrm{b}} + p_j - r_j \frac{(p_j^{\mathrm{b}})^2 + (q_j^{\mathrm{b}})^2}{v_j^2} \\
q_j^{\mathrm{b}} &= \sum_{k \in c(j)} q_k^{\mathrm{b}} + q_j - x_j \frac{(p_j^{\mathrm{b}})^2 + (q_j^{\mathrm{b}})^2}{v_j^2} \\
v_j^2 &= v_{e(j)}^2 - 2(r_j p_j^{\mathrm{b}} + x_j q_j^{\mathrm{b}}) \\
&\quad + (r_j^2 + x_j^2) \frac{(p_j^{\mathrm{b}})^2 + (q_j^{\mathrm{b}})^2}{v_{e(j)}^2},
\end{aligned}
\tag{7}
$$

where $\boldsymbol{p}$ and $\boldsymbol{q} \in \mathbb{R}^n$ are real and reactive power injections at each node, p_j^{b} and q_j^{b} are real and reactive power flows on the branch ending at node j, and $\boldsymbol{v} \in \mathbb{R}^n$ is voltage at each node. For any $\boldsymbol{p}$, $\boldsymbol{q}$ and substation voltage v_0, the voltage solution $\boldsymbol{v}$ of the DistFlow equations is unique [17].

Let $h_{v_j}(\boldsymbol{p}, \boldsymbol{q}, v_0)$ be the voltage solution of the DistFlow equations given $\boldsymbol{p}$, $\boldsymbol{q}$, and v_0. Then, the voltage $V_j^+(u)$ at next time step at node j is equal to $h_{v_j}(\boldsymbol{P}^+(u), \boldsymbol{Q}^+(u), v_0)$, which is a random variable. Now, we define a random variable $X^+(u)$ indicating network safety, i.e.,

$$
X^+(u) = \begin{cases} 1, & \text{if } V_j^+(u) \geq \underline{v} \ \forall j \in [n], \\ 0, & \text{otherwise.} \end{cases}
\tag{8}
$$

Note that $X^+(u)$ is a Bernoulli random variable. Then, the probability of network safety at the next time step under input $u(t+1) = u$ is the success probability of $X^+(u)$, which we denote $\theta^+(u)$. It is difficult to compute $\theta^+(u)$ in closed form. Instead, we propose a set of sufficient conditions to guarantee from a Monte Carlo simulation that $\theta^+(u)$ is above the desired safety probability $1 - \epsilon$ with the desired confidence level $1 - \beta$.

B. Confidence interval for success probability of a Bernoulli random variable

We first introduce the following Theorem from our recent work [6] on the confidence interval of the success probability of a Bernoulli random variable.

Theorem 1 (Theorem 1 of [6]). *Let n_s be the number of samples and $Y^{(1)}, \ldots, Y^{(n_s)}$ be the i.i.d. samples of a Bernoulli random variable Y with success probability $\theta > 0$. Denote the estimator of θ from the samples by $M_{n_s} := \sum_{i=1}^{n_s} Y^{(i)}/n_s$ and a realization by $\tilde{m}_{n_s}$. Then, $[1 - \epsilon, 1]$ is a confidence interval for θ with confidence level over $1 - \beta$ if the following inequalities hold*

$$
\begin{aligned}
&\tilde{m}_{n_s} > 1 - \epsilon, \\
&n_s > \ln\left(\frac{1}{\beta}\right) \frac{1}{(\tilde{m}_{n_s} + \epsilon)\ln(\tilde{m}_{n_s} + \epsilon) - (\tilde{m}_{n_s} + \epsilon - 1)}.
\end{aligned}
\tag{9}
$$

Since $X^+(u)$ is a Bernoulli random variable and $\theta^+(u)$ is its success probability, this theorem implies that we can verify if $[1 - \epsilon, 1]$ is a confidence interval of $\theta^+(u)$ with a certain confidence level by sampling $X^+(u)$. Specifically, the utility should sample n_s realizations of $X^+(u)$, compute the estimator $\tilde{m}_{n_s}$, and see if the inequalities (9) hold.

Next, we explain the procedure for how the utility samples a realization of $X^+(u)$.

1) Sample a realization of each of $\boldsymbol{P}^{\mathrm{L}+}$, $\boldsymbol{Q}^{\mathrm{L}+}$ from the joint probability distribution $f_{\boldsymbol{P}^L, \boldsymbol{Q}^L}^{t+1}$.
2) From the obtained realizations in the previous step, compute a realization of each of $\boldsymbol{P}^+(u)$, $\boldsymbol{Q}^+(u)$ using (6), a realization of $V_j^+(u) = h_{v_j}(\boldsymbol{P}^+(u), \boldsymbol{Q}^+(u), v_0)$ for all $j \in [n]$ using (7), and finally a realization of $X^+(u)$ using (8).

Note that the utility tracks the energy state $e^i(t)$ and the power $p^i(t)$ of all of the batteries so that it can accurately compute the anticipated one-step ahead net power consumption of the batteries $\boldsymbol{p}^{\mathrm{B}+}(u)$ using (5). It is also assumed that the utility can compute $\boldsymbol{p}^{\mathrm{D}+}(u), \boldsymbol{q}^{\mathrm{D}+}(u)$. Thus, the utility can obtain realizations of all of the random variables in step 2).

Now let $\tilde{x}^{(1)}, \ldots, \tilde{x}^{(n_s)}$ be the obtained realizations of $X^+(u)$ with $\tilde{m}_{n_s}$ as defined in Theorem 1. If $\tilde{m}_{n_s}$ and n_s satisfy the inequalities in (9), then we can conclude that the safety probability $\theta^+(u)$ is greater than or equal to the desired probability $1 - \epsilon$ with confidence level over $1 - \beta$. In the next section, we will introduce a constraint construction algorithm that iteratively conducts this test to obtain the maximum possible $\overline{u}$ for which the anticipated one-step ahead safety probability $\theta^+(\overline{u})$ satisfies the desired probabilistic safety conditions in Problem 1.

C. Constraint set construction

In this section, we explain the algorithm for the utility to construct a constraint set on the control command $u(t+1)$. This method is based on an assumption that the anticipated one-step ahead network safety $\theta^+(u)$ tends to decrease as u increases. This is intuitive since both the real and reactive net power consumption of the participating DERs at every
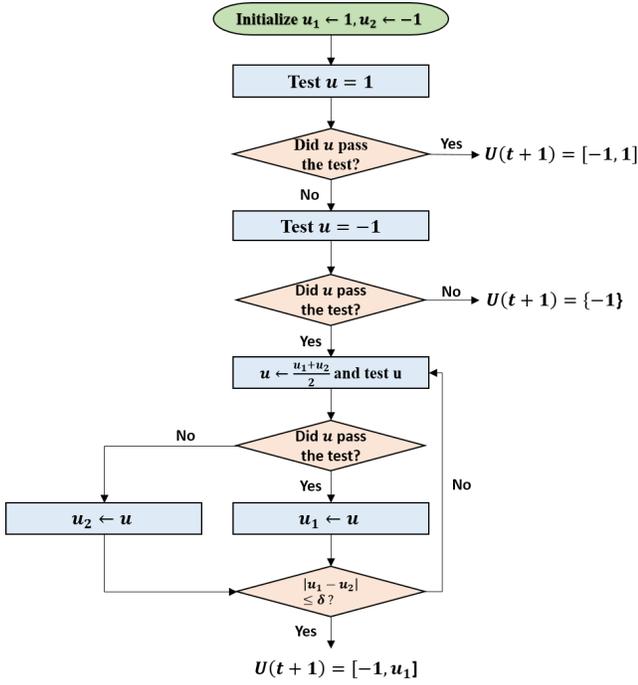
Fig. 3: Flowchart of the Bisection Method for the construction of the constraint set $\mathcal{U}(t+1) = [-1, \overline{u}]$.

node increase with u, which is likely to result in a lower voltage at each node. Also, this monotonicity assumption on $\theta^+(u)$ is justified in our recent work [6] by showing that the approximation of $\theta^+(u)$ obtained by solving the *LinDistFlow equations* from [16] (which approximate the DistFlow equations in (7)) is actually a decreasing function with respect to u.

Now suppose that $\theta^+(\overline{u}) \geq 1 - \epsilon$ holds. Then, under the monotonicity assumption, $\theta^+(u) \geq 1 - \epsilon$ also holds for any u in range $[-1, \overline{u}]$. Thus, the constraint set $\mathcal{U}(t+1) = [-1, \overline{u}]$ is a solution of Problem 1. Therefore, the utility needs to find an upper bound $\overline{u}$ which satisfies $\theta^+(\overline{u}) \geq 1 - \epsilon$. We know that if the inequalities (9) hold for the samples of $X^+(\overline{u})$, then $\theta^+(\overline{u}) \geq 1 - \epsilon$ also holds with the desired confidence level $1 - \beta$. Note that a larger constraint set $\mathcal{U}(t+1) = [-1, \overline{u}]$ leads to larger DER flexibility and potential improvement of the balancing service quality. To obtain the largest possible $\overline{u}$, the utility leverages the Bisection method, which is shown in Fig. 3.

Then, the aggregator should pick the control command $u(t+1)$ that maximizes the quality of the balancing service. Thus, the aggregator's control command can be computed as

$$u(t+1) = \underset{u \in \mathcal{U}(t)}{\arg\min} \left| \sum_{j=1}^{n} \left(p_j^{\mathrm{B}+}(u) + p_j^{\mathrm{D}+}(u) \right) - p_{\mathrm{ref}}(t+1) \right| \tag{10}$$

which minimizes the difference between the aggregate power consumption/production of the participating DERs and the reference signal.

V. CASE STUDY

In this section, we demonstrate the result of a case study in which we compare the proposed approach with two benchmark approaches.

A. Set-up

The 56-bus balanced radial distribution network from [18] is used. The real and reactive nominal power consumption at node j of this network are denoted by p_j^{Ln} and q_j^{Ln}, respectively.

We assume that there are only two types of participating DERs, batteries and TCLs. The TCLs switch their modes in reaction to the aggregator's command $u(t)$ by following the policy proposed in [6]. The total number of the TCLs is denoted by n^{T}. The entire DER population is distributed throughout the nodes so that the nominal real power consumption of the participating DERs at each node is $0.5 p_j^{\mathrm{Ln}}$. We denote by T^i the temperature and by m^i the mode of ith TCL. The mode of a TCL is 1 when it is ON and 0 when it is OFF. Then, the internal temperature dynamics of each TCL are

$$T^{i+} = a_{\mathrm{th}}^i T^i + (1 - a_{\mathrm{th}}^i)(T_a^i - b_{\mathrm{th}}^i m^i), \tag{11}$$

where T_a^i is the ambient temperature, and $a_{\mathrm{th}}^i := \exp(-\Delta t/(r_{\mathrm{th}}^i c_{\mathrm{th}}^i))$, $b_{\mathrm{th}}^i = r_{\mathrm{th}}^i p_{\mathrm{tr}}^i$ are the parameters related to thermal resistance, thermal capacitance and power transfer rate of the ith TCL. The controller should keep the internal temperature within the dead-band $[\underline{T}^i, \overline{T}^i]$. Also, we denote by p_{T}^i and q_{T}^i the rated real and reactive power consumption of the ith TCL. We assume every TCL has a constant lagging power factor ϕ^i and the rated reactive power consumption is $q_{\mathrm{T}}^i := \tan(\arccos \phi^i) p_{\mathrm{T}}^i.$[3] Also, we denote by $\mathcal{I}_j^{\mathrm{T}}$ the set of the indices of the TCLs connected to the node j.

We assume that the nominal real and reactive power consumption of the non-participating DERs and loads are $0.5 p_j^{\mathrm{Ln}}$ and $0.5 q_j^{\mathrm{Ln}}$. Also, we assume that the real and reactive power consumption of the non-participating DERs and loads $P_j^{\mathrm{L}}(t)$ and $Q_j^{\mathrm{L}}(t)$ follow truncated normal distributions $\mathcal{N}(\overline{p}_j^{\mathrm{L}}(t), (0.075 p_j^{\mathrm{Ln}})^2)$, $\mathcal{N}(\overline{q}_j^{\mathrm{L}}(t), (0.075 q_j^{\mathrm{Ln}})^2)$, where the means $\overline{p}_j^{\mathrm{L}}(t)$, $\overline{q}_j^{\mathrm{L}}(t)$ increase from $0.5 p_j^{\mathrm{Ln}}$, $0.5 q_j^{\mathrm{Ln}}$ to $0.65 p_j^{\mathrm{Ln}}$, $0.65 q_j^{\mathrm{Ln}}$ from 13.0h to 13.9h, are constant at $0.65 p_j^{\mathrm{Ln}}$, $0.65 q_j^{\mathrm{Ln}}$ from 13.9h to 14.1h, and linearly decrease to $0.5 p_j^{\mathrm{Ln}}$, $0.5 q_j^{\mathrm{Ln}}$ from 14.1h to 15.0h. These normal distributions are truncated to the ranges $[p_j^{\mathrm{Lmin}}, p_j^{\mathrm{Lmax}}] = [-0.05 p_j^{\mathrm{Ln}}, 0.7 p_j^{\mathrm{Ln}}]$, and $[q_j^{\mathrm{Lmin}}, q_j^{\mathrm{Lmax}}] = [-0.05 q_j^{\mathrm{Ln}}, 0.7 q_j^{\mathrm{Ln}}]$. Fig. 4 shows the plot of $\overline{p}_1^{\mathrm{L}}(t)$. Note that at every time step the means are are greater than or equal to the nominal power consumption of the non-participating DERs and loads, which makes the voltage at each node lower than in the nominal case; hence, this scenario is likely to lead to an under-voltage violations. The safe lower bound on the voltage is set to $\underline{v} = 0.95$ pu.

The reference signal is obtained from a scaled and shifted 2-hour segment of PJM's RegD frequency regulation signal

---

[3]The parameters for DERs are sampled from uniform distributions with the following intervals: $\overline{e}^i \in [6, 8]$ kWh, $\underline{p}^i \in [-3.5, -2.5]$ kW, $\overline{p}^i \in [2.5, 3.5]$ kW, $\eta_{\mathrm{c}}^i \in [0.85, 0.95]$, $\eta_{\mathrm{d}}^i \in [0.85, 0.95]$, $\theta_a^i \in [29, 31]$ °C, $c_{\mathrm{th}}^i \in [1.5, 2.5]$ kWh/°C, $r_{\mathrm{th}}^i \in [1.2, 2.5]$ °C/kW, $p_{\mathrm{tr}}^i \in [14, 18]$ kW, $\zeta^i \in [2.3, 2.7]$, $\theta_s^i \in [20, 25]$ °C, $\gamma^i \in [1.5, 2]$ °C, and $\phi^i \in [0.95, 0.99]$. TCLs parameters are consistent with air conditioners. Also, we set $\Delta t = 60$s, which is used for both the constraint set and controller computations.
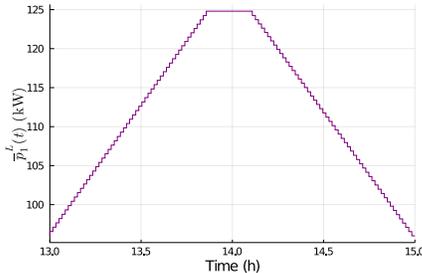
Fig. 4: Mean power consumption of the non-participating DERs and loads $\bar{p}_1^L(t)$ at node 1.

from [19], which can change every 2s. Since the control command is updated less frequently ($\Delta t = 60$s) than the RegD signal, we use a smoothed RegD signal as $p_{\text{ref}}(t)$ within our controller. Specifically, we assume that the aggregator receives the RegD signal one-minute ahead of real-time and averages the one-minute-ahead segment to compute $p_{\text{ref}}(t)$. We recognize that in practice the RegD signal is not known in advance and plan to develop a more realistic approach in future work. We emphasize that though the controller uses the smoothed signal as its reference signal, we still compute all of our performance metrics using the original RegD signal.

Last, we introduce the benchmark approaches to which we will compare our proposed method. The first is a simple tracking controller that ignores network safety. It chooses the optimal input $u_{\text{opt}}(t)$ to track $p_{\text{ref}}(t)$ by solving

$$u_{\text{opt}}(t+1) = \arg\min_{u \in [-1,1]} \left| \sum_{j=1}^{n} \left(p_j^{\text{B}+}(u) + p_j^{\text{D}+}(u) \right) - p_{\text{ref}}(t+1) \right|.$$

The comparison between the optimal tracking controller and our proposed method is expected to show the necessity of incorporating the constraint set to achieve network safety.

The second approach is an OPF approach that solves (12) in the Appendix at every time step to obtain the optimal power consumption/production of every DER while satisfying all of the DER and network constraints. This controller can observe the network's state and directly controls the power consumption/production of each participating DER. Thus, it has more degrees of freedom in control and also has more information on the DERs and the network than the other benchmark approach or our proposed method. However, it can be more conservative since the network safety constraint is deterministic and must be satisfied at all times.

B. Results

Here, we describe the results of our case study. Fig. 5 plots the obtained aggregate power $p_{\text{agg}}(t)$ of the participating DERs and the minimum voltage $\min_j v_j(t)$ amongst all of the nodes from all three algorithms. For our proposed approach, we consider two different $\epsilon = 0.1, 0.05$. Table I summarizes the tracking performance, specifically the RMSE of $p_{\text{agg}(t)}$ from the RegD signal (i.e., the reference signal in the top set of plots in Fig. 5), and the observed safety probability, which is computed as the portion of time steps

TABLE I: Comparison of controllers in terms of performance and safety

	Track Ctrl Benchmark	OPF Benchmark	Proposed Approach $\epsilon = 0.1$	$\epsilon = 0.05$
RMSE (kW)	415.0	650.0	569.3	585.7
Safety Probability	0.816	1.0	0.95	0.983

during which the network was safe over at all of the time steps during the simulation.

Even though the tracking controller benchmark is the best in terms of tracking performance, it frequently leads to under-voltage violations. This clearly shows the necessity of the constraint set on the aggregator's control command. In contrast, while the OPF benchmark succeeds in preventing under-voltage violations at all time steps, the tracking performance is significantly reduced. This shows that, even with direct control of the DERs' power consumption/production and measurements of the DERs' and network's states, it is impossible to develop a safety-guaranteed algorithm without a significant reduction in balancing service quality.

The performance of our proposed approach exhibits a good trade-off between performance and network safety, as compared to the other approaches. As shown in Table I the chance constraint (1) is satisfied by the proposed approach for both choices of ϵ. Also, its tracking performance is better than the OPF benchmark. This implies that, if some level of network safety violation is allowed (which is reasonable for distribution network where voltages do not need to be perfectly regulated), our algorithm could be a good compromise between a grid-agnostic approach and a deterministic grid-aware approach.

VI. CONCLUSION

In this paper, we proposed an extension of our recent work [6] to incorporate batteries within our framework developed to coordinate DERs to provide grid balancing services while achieving network safety with probabilistic guarantees. We developed an appropriate power control policy for batteries to react to the aggregator's control command and we showed how to compute a one-step ahead constraint set on the aggregator's control command to ensure the satisfaction of probabilistic network safety.

As possible extensions, we hope to incorporate other types of DERs such as electric vehicles and solar photovoltaics into our framework. Moreover, we plan to extend the framework to enable multi-dimensional aggregator control commands, which would add more degrees of freedom in control, potentially improving performance and network safety.

REFERENCES

[1] Federal Energy Regulatory Commission, "Notice inviting post-technical conference comments," Tech. Rep. Docket No. RM18-9-000, Apr. 2018. [Online]. Available : https://cms.ferc.gov/sites/default/files/2020-09/Notice-for-Comments-on-NOPR-RM18-9.pdf.

[2] E. Dall'Anese, S. Guggilam, A. Simonetto, Y. C. Chen, and S. Dhople, "Optimal regulation of virtual power plants," *IEEE Trans. Power Syst.*, vol. 33, no. 2, pp. 1868–1881, 2017.

[3] A. Bernstein and E. Dall'Anese, "Real-time feedback-based optimization of distribution grids: A unified approach," *IEEE Trans. Control Netw. Syst.*, vol. 6, no. 3, pp. 1197–1209, 2019.

(a) Tracking Controller Benchmark   (b) OPF Benchmark   (c) Proposed Approach ($\epsilon = 0.1$)   (d) Proposed Approach ($\epsilon = 0.05$)
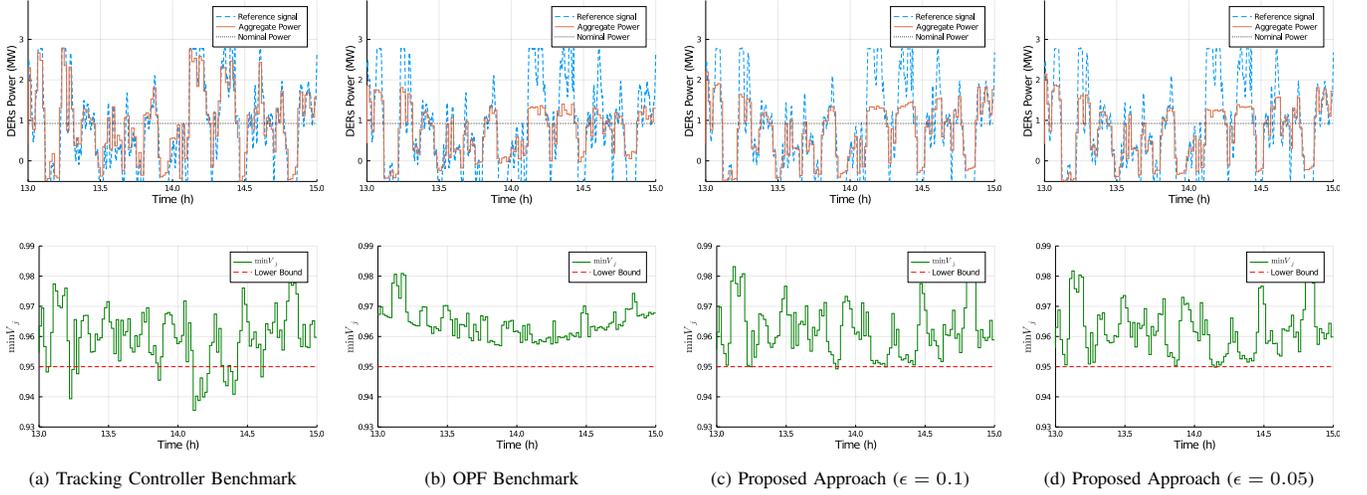
Fig. 5: The reference tracking performance (top) and the minimum voltages amongst all network nodes for the two benchmark approaches (a) and (b), and our proposed approach with two choices of ϵ (c) and (d).

[4] E. Vrettos and G. Andersson, "Combined load frequency control and active distribution network management with thermostatically controlled loads," in *IEEE SmartGridComm*, 2013, pp. 247–252.

[5] Federal Energy Regulatory Commission, "FERC order no. 2222: Participation of distributed energy resource aggregations in markets operated by regional transmission organizations and independent system operators." https://www.ferc.gov/sites/default/files/2020-09/E-1_0.pdf, sep 2020.

[6] S. Jang, N. Ozay, and J. Mathieu, "Probabilistic constraints construction for network-safe thermostatically controlled loads control," https://web.eecs.umich.edu/~necmiye/pubs/JangOM_j22.pdf, 2022.

[7] S. C. Ross, N. Ozay, and J. L. Mathieu, "Coordination between an aggregator and distribution operator to achieve network-aware load control," in *IEEE Milan PowerTech*, 2019.

[8] S. Ross and J. Mathieu, "Strategies for network-safe load control with a third-party aggregator and a distribution operator," *IEEE Trans. Power Syst.*, vol. 36, no. 4, pp. 3329–3339, 2021.

[9] S. Jang, N. Ozay, and J. L. Mathieu, "Large-scale invariant sets for safe coordination of thermostatic loads," in *Proc. Amer. Ctrl. Conf.*, 2021, pp. 4163–4170.

[10] K. Petrou, M. Z. Liu, A. T. Procopiou, L. F. Ochoa, J. Theunissen, and J. Harding, "Operating envelopes for prosumers in lv networks: A weighted proportional fairness approach," in *IEEE PES Innovative Smart Grid Technologies Europe*, 2020, pp. 579–583.

[11] Y. Yi and G. Verbič, "Fair operating envelopes under uncertainty using chance constrained optimal power flow," *Electric Power Systems Research*, vol. 213, p. 108465, 2022.

[12] J. S. Russell, P. Scott, and A. Attarha, "Stochastic shaping of aggregator energy and reserve bids to ensure network security," *Electric Power Systems Research*, vol. 212, p. 108418, 2022.

[13] H. D. Nguyen, K. Dvijotham, and K. Turitsyn, "Constructing convex inner approximations of steady-state security regions," *IEEE Trans. Power Syst.*, vol. 34, no. 1, pp. 257–267, 2018.

[14] D. Lee, K. Turitsyn, D. K. Molzahn, and L. A. Roald, "Robust ac optimal power flow with robust convex restriction," *IEEE Trans. Power Syst*, vol. 36, no. 6, pp. 4953–4966, 2021.

[15] N. Nazir and M. Almassalkhi, "Grid-aware aggregation and realtime disaggregation of distributed energy resources in radial networks," *IEEE Trans. Power Syst.*, 2021.

[16] M. E. Baran and F. F. Wu, "Network reconfiguration in distribution systems for loss reduction and load balancing," *IEEE Power Engineering Review*, vol. 9, no. 4, pp. 101–102, 1989.

[17] H.-D. Chiang and M. E. Baran, "On the existence and uniqueness of load flow solution for radial distribution power networks," *IEEE Trans. Circuits Syst.*, vol. 37, no. 3, pp. 410–416, 1990.

[18] S. Bolognani and S. Zampieri, "On the existence and linear approximation of the power flow solution in power distribution networks," *IEEE Trans. Power Syst.*, vol. 31, no. 1, pp. 163–172, 2015.

[19] PJM, "RTO regulation signal data for 7.19.2019 & 7.20.2019.xls," https://www.pjm.com/markets-and-operations/ancillary-services.aspx, accessed: 2019-10-22.

APPENDIX

A. OPF Benchmark Approach

Here, we introduce the OPF Benchmark optimization formulation, which is solved at each time step. The main decision variables are the charging and discharging power p_c^{i+} and p_d^{i+} of the batteries, and the mode of the TCLs m^{i+} at the next time step. The formulation includes all constraints on the states of each DER. To reduce the computational complexity of the optimization problem, we leverage the linearized power flow equations developed in [2]. Note that this approach finds a solution that is network-safe even under the maximum real and reactive power consumption of the non-participating DERs and loads p_j^{Lmax} and q_j^{Lmax}. Thus, the solution guarantees network safety.

$$\min_{p_c^{i+}, p_d^{i+}, m^{i+}} \left| \sum_{j=1}^{n} \left(p_j^{\text{B}+} + p_j^{\text{D}+} \right) - p_{\text{ref}}(t+1) \right|$$

$$\text{s.t.} \quad p_j^{\text{B}+} = \sum_{i \in \mathcal{I}_j^{\text{B}}} \left(p_c^{i+} + p_d^{i+} \right) \qquad \forall j \in [n]$$

$$p_j^{\text{D}+} = \sum_{i \in \mathcal{I}_j^{T}} p_{\text{T}}^i m^{i+} \qquad \forall j \in [n]$$

$$p_j^+ = p_j^{\text{B}+} + p_j^{\text{D}+} + p_j^{\text{Lmax}} \qquad \forall j \in [n]$$

$$q_j^+ = p_j^{\text{D}+} + q_j^{\text{Lmax}} \qquad \forall j \in [n]$$

Constraints (3) on $e^{i+}, p_c^{i+},$ and $p_d^{i+} \quad \forall i \in [n^{\text{B}}]$

Battery's energy state dynamics (2) $\quad \forall i \in [n^{\text{B}}]$

TCLs' temperature dynamics (11) $\quad \forall i \in [n^{\text{T}}]$

TCLs' temperature dead-band $\quad \forall i \in [n^{\text{T}}]$

$$\boldsymbol{v}^+ = A_{\text{lin}} \boldsymbol{p}^+ + B_{\text{lin}} \boldsymbol{q}^+ + c_{\text{lin}}$$

$$\underline{v} \leq \boldsymbol{v}^+.$$